AMERICAN SOCIETY FOR MICROBIOLOGY | Journal of Virology

Protective Effects of Glutamine Antagonist 6-Diazo-5-Oxo-L-Norleucine in Mice with Alphavirus Encephalomyelitis

Sivabalan Manivannan,[a]* Victoria K. Baxter,[a,b] Kimberly L. W. Schultz,[a]* Barbara S. Slusher,[c] Diane E. Griffin[a]

W. Harry Feinstone Department of Molecular Microbiology and Immunology, Johns Hopkins Bloomberg School of Public Health,[a] Department of Molecular and Comparative Pathobiology, Johns Hopkins University School of Medicine,[b] and Brain Science Institute, Department of Neurology, Johns Hopkins University School of Medicine,[c] Baltimore, Maryland, USA

ABSTRACT

Inflammation is a necessary part of the response to infection but can also cause neuronal injury in both infectious and autoimmune diseases of the central nervous system (CNS). A neurovirulent strain of Sindbis virus (NSV) causes fatal paralysis in adult C57BL/6 mice during clearance of infectious virus from the CNS, and the virus-specific immune response is implicated as a mediator of neuronal damage. Previous studies have shown that survival is improved in T-cell-deficient mice and in mice with pharmacological inhibition of the inflammatory response and glutamate excitotoxicity. Because glutamine metabolism is important in the CNS for the generation of glutamate and in the immune system for lymphocyte proliferation, we tested the effect of the glutamine antagonist DON (6-diazo-5-oxo-L-norleucine) on the outcome of NSV infection in mice. DON treatment for 7 days from the time of infection delayed the onset of paralysis and death. Protection was associated with reduced lymphocyte proliferation in the draining cervical lymph nodes, decreased leukocyte infiltration into the CNS, lower levels of inflammatory cytokines, and delayed viral clearance. *In vitro* studies showed that DON inhibited stimulus-induced proliferation of lymphocytes. When *in vivo* treatment with DON was stopped, paralytic disease developed along with the inflammatory response and viral clearance. These studies show that fatal NSV-induced encephalomyelitis is immune mediated and that antagonists of glutamine metabolism can modulate the immune response and protect against virus-induced neuroinflammatory disease.

IMPORTANCE

Encephalomyelitis due to infection with mosquito-borne alphaviruses is an important cause of death and of long-term neurological disability in those who survive infection. This study demonstrates the role of the virus-induced immune response in the generation of neurological disease. DON, a glutamine antagonist, inhibited the proliferation of lymphocytes in response to infection, prevented the development of brain inflammation, and protected mice from paralysis and death during treatment. However, because DON inhibited the immune response to infection, clearance of the virus from the brain was also prevented. When treatment was stopped, the immune response was generated, brain inflammation occurred, virus was cleared, and mice developed paralysis and died. Therefore, more definitive treatment for alphaviral encephalomyelitis should inhibit virus replication as well as neuroinflammatory damage.

Sindbis virus (SINV) is a mosquito-borne, enveloped, positive-strand RNA virus of the genus *Alphavirus* in the family *Togaviridae*. SINV causes rash and arthritis in humans and causes acute encephalomyelitis in mice by infecting neurons (1, 2). Many factors, including age, genetic background, virus strain, route of inoculation, and immune competency, determine the outcome of infection in mice (3–8). A neuroadapted strain of SINV (NSV) causes progressive paralysis and death of adult C57BL/6 mice and provides a model for understanding the pathogenesis and treatment of acute fatal viral encephalomyelitis (9). Both direct T-cell-mediated cytotoxicity and glutamate excitotoxicity have been implicated in neuronal damage during acute infection (8, 10–13).

Survival after NSV infection is improved in mice deficient in $CD4^+$ or $CD8^+$ T-cell responses (7, 8), and treatment with antagonists of α-amino-3-hydroxy-5-methyl-4-isoxazole propionic acid (AMPA) glutamate receptors also protects from fatal disease. However, an unanticipated effect of the AMPA receptor antagonists was inhibition of the antiviral immune response that resulted in decreased central nervous system (CNS) inflammation and delayed virus clearance (11, 12). Because both the adaptive antiviral immune response and glutamate excitotoxicity are potential mediators of neuronal cell death in NSV infection (7, 8, 10–12), we investigated the protective effects of glutamine antagonists anticipated to potentially affect both lymphocyte proliferation and glutamate synthesis.

In the immune system, T cells preferentially use glutamine rather than glucose for metabolic needs during growth and proliferation (14, 15). Increased glutamine uptake and metabolism are characteristic of rapidly dividing cells such as activated T cells

Received 27 May 2016 **Accepted** 28 July 2016

Accepted manuscript posted online 3 August 2016

Citation Manivannan S, Baxter VK, Schultz KLW, Slusher BS, Griffin DE. 2016. Protective effects of glutamine antagonist 6-diazo-5-oxo-L-norleucine in mice with alphavirus encephalomyelitis. J Virol 90:9251–9262. doi:10.1128/JVI.01045-16.

Editor: S. Perlman, University of Iowa

Address correspondence to Diane E. Griffin, dgriffi6@jhu.edu.

* Present address: Sivabalan Manivannan, 1871, Chicago, Illinois, USA; Kimberly L. W. Schultz, U.S. Food and Drug Administration, Silver Spring, Maryland, USA.

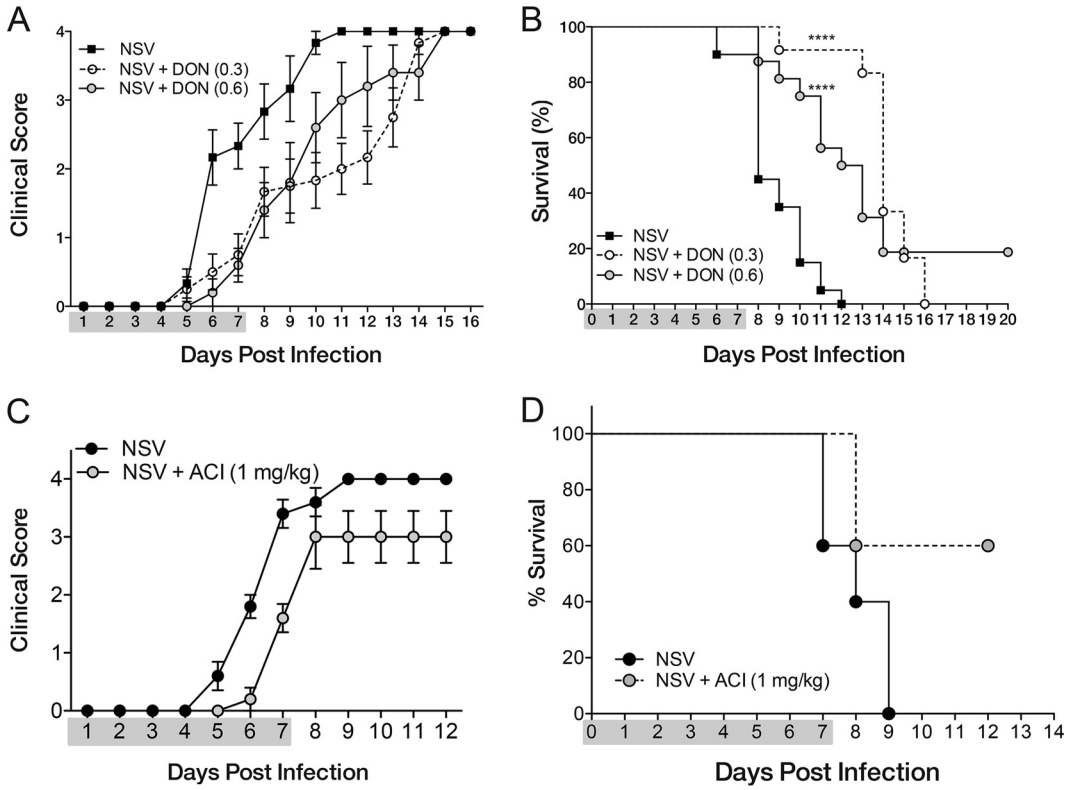

FIG 1 DON treatment protects mice from NSV-induced acute disease. Six- to eight-week-old C57BL/6 mice were infected with 1,000 PFU of NSV intracerebrally and treated every 24 h intraperitoneally with the glutamine antagonist DON (0.3 mg/kg or 0.6 mg/kg), ACI (1 mg/kg), or PBS (100 to 200 μl) from the time of infection through day 7. (A) Clinical scores of treated and untreated mice ($n = 6$ for NSV, $n = 12$ for DON at 0.3 mg/kg, and $n = 5$ DON at 0.6 mg/kg). Clinical scores were as follows: 0 for no clinical signs, 1 for mild weakness, 2 for paralysis of one hind limb, 3 for paralysis of both hind limbs, and 4 for death. (B) Mortality of treated and untreated mice ($n = 20$ for NSV, $n = 12$ for DON at 0.3 mg/kg, and $n = 15$ for DON at 0.6 mg/kg). For PBS-treated mice (NSV), the median time of survival was 8 days, while DON-treated mice had median survival times of 14 days (0.3 mg/kg) and 12 days (0.6 mg/kg). ****, $P < 0.0001$ as determined by a log rank (Mantel-Cox) survival test. Data are pooled from results of 2 independent experiments. (C and D) Clinical scores (C) and mortality (D) of ACI-treated ($n = 5$) and PBS-treated ($n = 5$) mice. Gray shading designates the drug treatment period.

and certain cancer cells (16). Proliferating T cells require millimolar concentrations of extracellular glutamine for growth and cell cycle progression, and T cells stimulated in glutamine-deprived media fail to expand in size, replicate their DNA, or enter S phase (16, 17). Additionally, silencing of key enzymes involved in glutamine metabolism, such as phosphate-activated glutaminase (GLS1), which is upregulated during T-cell activation, completely inhibits the proliferation of human T cells (18). In the nervous system, glutamine is required for the synthesis of the primary excitatory neurotransmitter glutamate, and excess production can result in excitotoxic damage to neurons (19, 20). Therefore, the availability and metabolism of glutamine could be a critical metabolic bottleneck that might be pharmacologically exploited to modulate the response to and prevent neuronal damage during neuroinflammatory diseases such as NSV-induced acute encephalomyelitis.

To determine if pharmacological inhibition of glutamine metabolism can protect mice from NSV-induced fatal paralysis, we treated mice with the glutamine antagonist DON (6-diazo-5-oxo-L-norleucine). DON is a *Streptomyces*-derived antimetabolite that competitively and irreversibly binds to the active sites of many glutamine-utilizing enzymes, permanently inhibiting their catalytic activities (21). DON was discovered in the 1950s and initially developed as a cancer chemotherapeutic (22, 23). Clinical trials from the 1980s showed that DON was effective against tumor cells, but prolonged treatment resulted in substantial toxicity, so further development was not pursued (24–27). However, recently, DON has been shown to inhibit lymphocyte proliferation (28), inhibit graft rejection (29), decrease SINV-induced memory impairment (30), and improve outcomes for mice with cerebral malaria (31), suggesting its use as an immunomodulator.

In our studies, treatment with DON inhibited the adaptive immune response to NSV infection and delayed the onset of acute fatal encephalomyelitis. DON-induced suppression of the antiviral immune response resulted in decreased CNS inflammation and prevented virus clearance. However, with the cessation of treatment, an antiviral immune response was generated along with viral clearance and fatal paralysis, confirming the role of the immune response in disease pathogenesis.

MATERIALS AND METHODS

Cell culture and drugs. BHK cells were grown in Dulbecco's modified Eagle's medium (DMEM) supplemented with 10% fetal bovine serum (FBS), penicillin (Pen), streptomycin (Strep), and 2 mM glutamine (Invitrogen). Primary lymphocytes were grown in DMEM supplemented with 10% dialyzed FBS, Pen-Strep, glutamine, and 50 μM β-mercaptoethanol (Sigma). Glutamine-deficient DMEM was used in certain experiments. All cells were grown at 37°C with 5% CO_2.

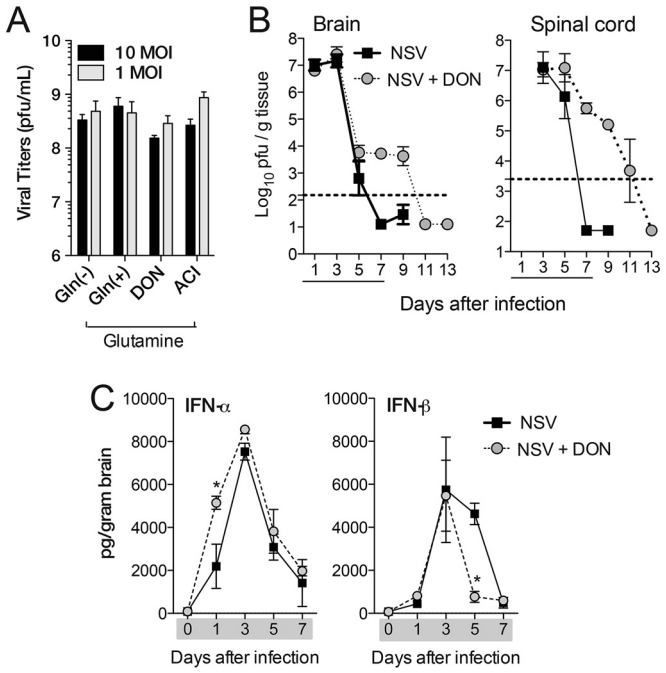

FIG 2 Effect of glutamine deprivation on virus replication and interferon induction. (A) Virus produced after *in vitro* NSV infection at MOIs of 1 and 10 of BHK cells in either complete medium [Gln(+)], glutamine-deficient medium [Gln(−)], or complete medium with the glutamine antagonist DON (100 μM) or ACI (100 μM). BHK cells were glutamine and serum starved for 24 h before infection with NSV. Supernatant fluids were collected 24 h after infection and assayed for plaque formation on BHK cells. (B) Viral titers from the brains and spinal cords of PBS-treated (NSV) and DON-treated (NSV + DON) (0.6 mg/kg for brain and 0.3 mg/kg for spinal cord) mice. Error bars represent standard errors of the geometric mean titers from three biological replicates (A) or three mice (B). The dotted line represents the limit of detection of the plaque assay. Data are representative of results from at least two independent experiments (B). (C) Levels of IFN-α and IFN-β in the brains of PBS-treated (NSV) and DON-treated (NSV + DON) (0.3 mg/kg) mice as determined by EIAs. Data represent the means ± standard errors of the means of data for 3 mice. Gray shading or underlining designates the drug treatment period. *, $P < 0.05$; ***, $P < 0.001$ (as determined by one-way ANOVA with Dunnett's posttest [A] or two-way ANOVA with a Bonferroni posttest [B and C]).

The glutamine antagonists DON (Sigma) and acivicin (ACI; Sigma) were solubilized in sterile phosphate-buffered saline (PBS) to prepare 100 mM stock solutions. Working dilutions were made in medium for *in vitro* experiments or in sterile PBS for *in vivo* experiments. Stock solutions were stored at −80°C, and fresh working solutions were made for each use.

Virus and virus assays. NSV (9) was grown in BHK cells in DMEM supplemented with 1% FBS, Pen-Strep, and glutamine. Supernatant fluid was collected 24 h after infection, filtered through a 40-μm filter, and stored in aliquots at −80°C. For plaque assays, supernatant fluids and tissue homogenates (20%) were serially diluted in DMEM with 1% FBS, inoculated onto BHK cells, incubated at 37°C for 1 h, washed, and overlaid with agar (1.2% Bacto agar, minimal essential medium [MEM], 1% FBS). After incubation for 48 h, cells were stained with neutral red, and plaques were counted.

Animal infection, treatment, and tissue harvest. Six- to eight-week-old female C57BL/6J mice (Jackson Laboratory) were inoculated intracerebrally with 1,000 PFU NSV in 20 μl of Hanks' balanced salt solution (HBSS) or PBS under light isoflurane anesthesia. Mice were treated daily with 100 μl of PBS, 0.3 or 0.6 mg/kg of body weight of DON, or 1 mg/kg ACI in 100 to 200 μl PBS intraperitoneally from the time of infection through day 7 after infection. Mice were scored daily for disease as follows: 0 for no signs of weakness, 1 for mild weakness and hunched posture, 2 for paralysis of one hind limb, 3 for paralysis of both hind limbs, and 4 for death.

For tissue collection, mice were deeply anesthetized, and blood was collected by cardiac puncture into serum separator tubes (BD Microtainer). Mice were then perfused with ice-cold PBS. Brain, spinal cord, and cervical lymph node tissues were collected and either used fresh for cell analysis or snap-frozen and stored at −80°C for plaque assays and RNA extraction. All studies were done in accordance with protocols approved by the Johns Hopkins University Animal Care and Use Committee.

qRT-PCR analysis. RNA was extracted from frozen brains by using the RNeasy lipid tissue kit (Qiagen). Extracted RNA was diluted to 1 μg/μl, and 2 μg was reverse transcribed by using the High Capacity cDNA reverse transcription kit (Applied Biosystems). The cDNA (2.5 μl) was analyzed for the following mRNAs by TaqMan reverse transcription-quantitative PCR (qRT-PCR): interleukin-1β (IL-1β) (mm0434228_m1), IL-6 (mm00466190_m1), tumor necrosis factor alpha (TNF-α) (mm99999068_m1), IL-12, CCL2 (mm00441242_m1), CCL5 (mm01302427_m1), CXCL10 (mm99999072_m1), IL-10 (mm00439616_m1), transforming growth factor β (TGF-β), IL-4 (mm00445259_m1), gamma interferon (IFN-γ) (mm00801778_m1), T-bet (mm00450960_m1), GATA3 (mm00484683_m1), FoxP3 (mm00475162_

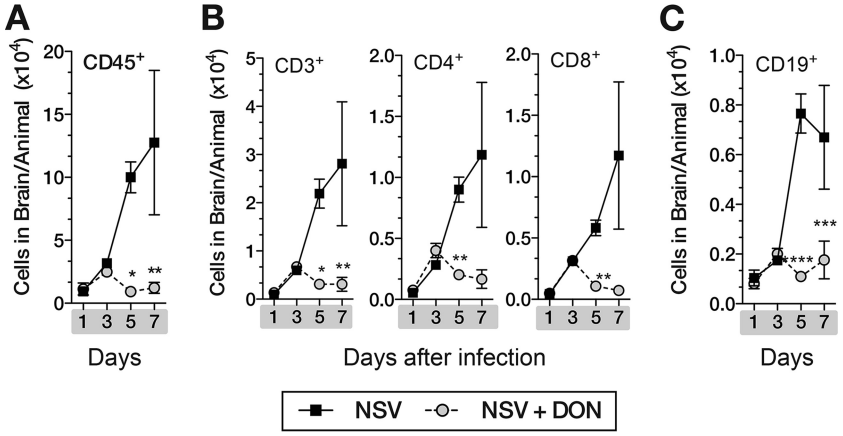

FIG 3 DON-treated mice have decreased leukocyte infiltration into the brain. Inflammation in the brains of NSV-infected DON-treated and PBS-treated mice (days 0 to 7) was evaluated by flow cytometry. Mononuclear cells were isolated from brains of mice ($n = 3$/group) by Percoll gradient centrifugation, and numbers of $CD45^+$ (A); $CD3^+$, $CD4^+$, and $CD8^+$ (B); and $CD19^+$ (C) cells/brain were determined. Data are representative of results from at least three independent experiments. *, $P < 0.05$; **, $P < 0.01$; ***, $P < 0.001$ (as determined by two-way ANOVA with a Bonferroni posttest).

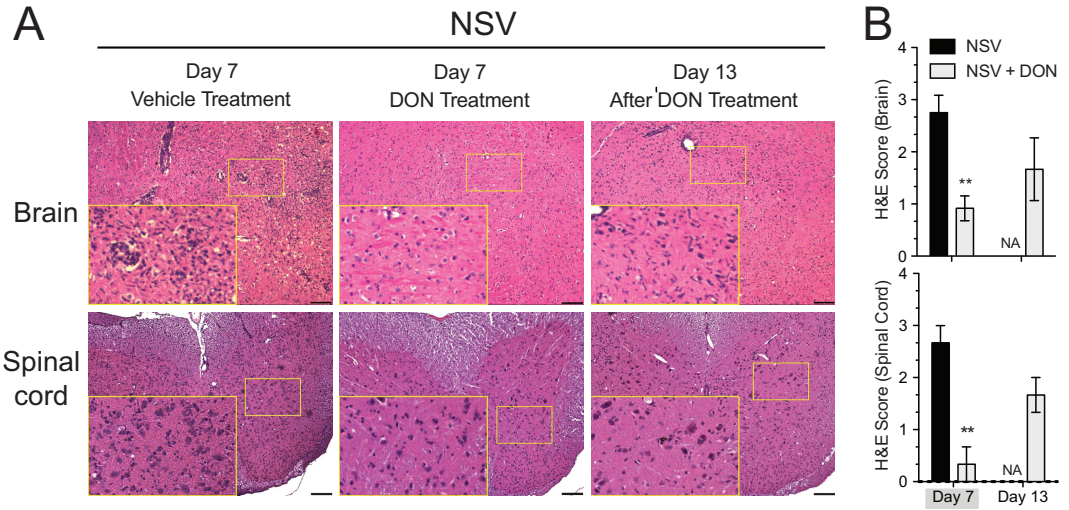

FIG 4 Leukocytes appear in the brains and spinal cords of treated mice after DON treatment is stopped. (A) Representative H&E-stained brain (top) and spinal cord (bottom) sections from day 7 (treated and untreated) and day 13 (after DON treatment was stopped at day 7). (B) H&E-stained sections were scored as follows: 0 for no inflammation, 1 for one or two occasional inflammatory foci, 2 for moderate foci in <50% of 10× fields, and 3 for moderate to severe foci in >50% of 10× fields. A score of +1 was given for abundant cellularity. Mice were treated with PBS or 0.3 mg/kg of DON once daily through day 7. Gray shading under the *x* axis identifies the drug treatment period. Bar = 100 μm. Error bars represent standard errors of the means of data for three mice per time point per group. **, $P < 0.01$ (as determined by one-way ANOVA). NA, not applicable.

m1), and RoRc-γ (mm01261022_m1) (Applied Biosystems). Data were acquired on a 7500 real-time PCR machine (Applied Biosystems) and analyzed by using Excel software. Data from all samples were normalized to values for rodent glyceraldehyde-3-phosphate dehydrogenase (GAPDH; Applied Biosystems), and fold induction was calculated relative to values for RNA from brains of uninfected mice.

Histopathology and immunohistochemistry. Deeply anesthetized mice were perfused with 20 ml ice-cold PBS before being perfused with 40 ml of ice-cold 4% paraformaldehyde (PFA). Spinal cords and brains cut into 2-mm coronal sections were fixed with 4% PFA overnight at 4°C, rinsed with cold PBS, embedded in paraffin, sectioned (10 μm), and stained with hematoxylin and eosin (H&E) by the Johns Hopkins Hospital Pathology Laboratory. Coded H&E-stained sections were scored as follows: 0 for no inflammation, 1 for one or two occasional inflammatory foci, 2 for moderate foci in <50% of 10× fields, and 3 for moderate to severe foci in >50% of 10× fields. A score of +1 was given for abundant cellularity.

For immunohistochemistry, sections were heated at 58°C for 10 min and then rehydrated through solutions containing xylene, 100% ethanol, 95% ethanol, 70% ethanol, and deionized water. Sections were boiled in citrate buffer (10 mM citrate [pH 6] with 0.05% Tween 20) for 10 min, cooled, and washed in PBS. Sections were blocked with 5% normal goat serum in Neuropore (Trevigen) and then stained with antibodies against NSV (1:100, polyclonal) (2), CD3 (1:100, SP7 clone; Abcam), or NeuN (1:50; Millipore) overnight at 4°C in a humidified chamber. Slides were washed with PBST (PBS with 0.05% Tween 20) and then incubated with the appropriate fluorescently conjugated (Alexa 594 or Alexa 488; Invitrogen) secondary antibodies diluted in Neuropore (1:200) for 1 h at room temperature (RT). Slides were washed in PBST, immersed in 0.1% Sudan black in 70% ethanol for 20 min, and washed. Sections were mounted by using ProLong Gold with 4′,6-diamidino-2-phenylindole (DAPI) (Invitrogen) for 24 h in the dark at RT, and images were obtained by using a Nikon 90i microscope with Volocity software. Numbers of cells were counted in 10 random fields per coded tissue section at a ×20 magnification and averaged.

Isolation and analysis of mononuclear cells from brains and cervical lymph nodes. Mononuclear cells were isolated from brains as described previously (32). Briefly, brains were homogenized in isotonic Percoll (9 parts Percoll [GE Healthcare] and 1 part 10× HBSS [Mediatech]), treated with DNase I (Sigma) for 30 min at RT, and layered onto a 30 to 70% discontinuous Percoll gradient. After centrifugation at 500 × *g* for 30 min, mononuclear cells at the interface were collected. Lymph nodes were placed onto a 40-μm-mesh filter in a cold petri dish containing RPMI, and cells were disassociated by using the blunt end of a syringe piston.

For flow cytometry, cells were stained with Aqua Live/Dead dye (Invitrogen), washed with fluorescence-activated cell sorter (FACS) buffer (PBS with 1% bovine serum albumin [BSA] and 2 mM EDTA), blocked with Fc Block (BD Biosciences), and stained with fluorescently conjugated antibodies (BD Biosciences) against mouse CD3 (allophycocyanin [APC]-Cy7, 17A2 clone), CD45 (fluorescein isothiocyanate [FITC], 30-F11 clone), CD4 (peridinin chlorophyll protein [PerCP]-Cy5.5, RM4-5 clone), CD8 (phycoerythrin [PE]-Cy7, 53-6.7 clone), and CD19 (APC, 1D3 clone). Washed cells were resuspended in 400 μl FACS buffer, and 50 μl of CountBrite beads (Invitrogen) was added. Cells were analyzed on a FACSCanto II flow cytometer to calculate absolute numbers of live cells.

BrdU incorporation. A bromodeoxyuridine (BrdU; Sigma) stock (50 mg/ml) was prepared in PBS and stored in aliquots at −80°C. BrdU (2 mg in 200 μl) was administered intraperitoneally on days 4 and 5 after NSV infection. After 8 h, superficial cervical lymph nodes were removed, and viability was determined as described above. Cells were fixed, permeabilized (BD Cytofix/Cytoperm), incubated in nuclear staining buffer (0.5% Triton X-100, 1% BSA, 2 mM EDTA) for 10 min, fixed by using Cytofix/Cytoperm buffer, and then incubated in DNase (Sigma) (30 μg/10^6 cells) for 1 h at 37°C. Cells were stained with FITC-conjugated antibody to BrdU (BD Biosciences) for 20 min at RT, washed, and analyzed on a FACSCanto II flow cytometer.

***In vitro* T-cell analysis.** $CD3^+$ lymphocytes were purified from the spleens of uninfected adult C57BL/6J mice by using a Pan T-cell Isolation kit (Miltenyi Biotec). For activation, flat-bottom 96-well plates were coated with anti-CD3 (5 μg/ml; 145-2C11 clone) and anti-CD28 (2.5 μg/ml; 37.51 clone) (eBioscience) for 2 h at 37°C and washed. Prior to culture, lymphocytes were stained with carboxyfluorescein succinyl ester (CFSE; Invitrogen) in PBS with 0.1% BSA for 5 min at 37°C, washed, and then added at a density of 10^5 cells/well. Cells were cultured in glutamine-free or complete medium (DMEM, 10% dialyzed FBS, 2 mM glutamine, nonessential amino acids [NEAAs], 25 mM HEPES) in the presence or

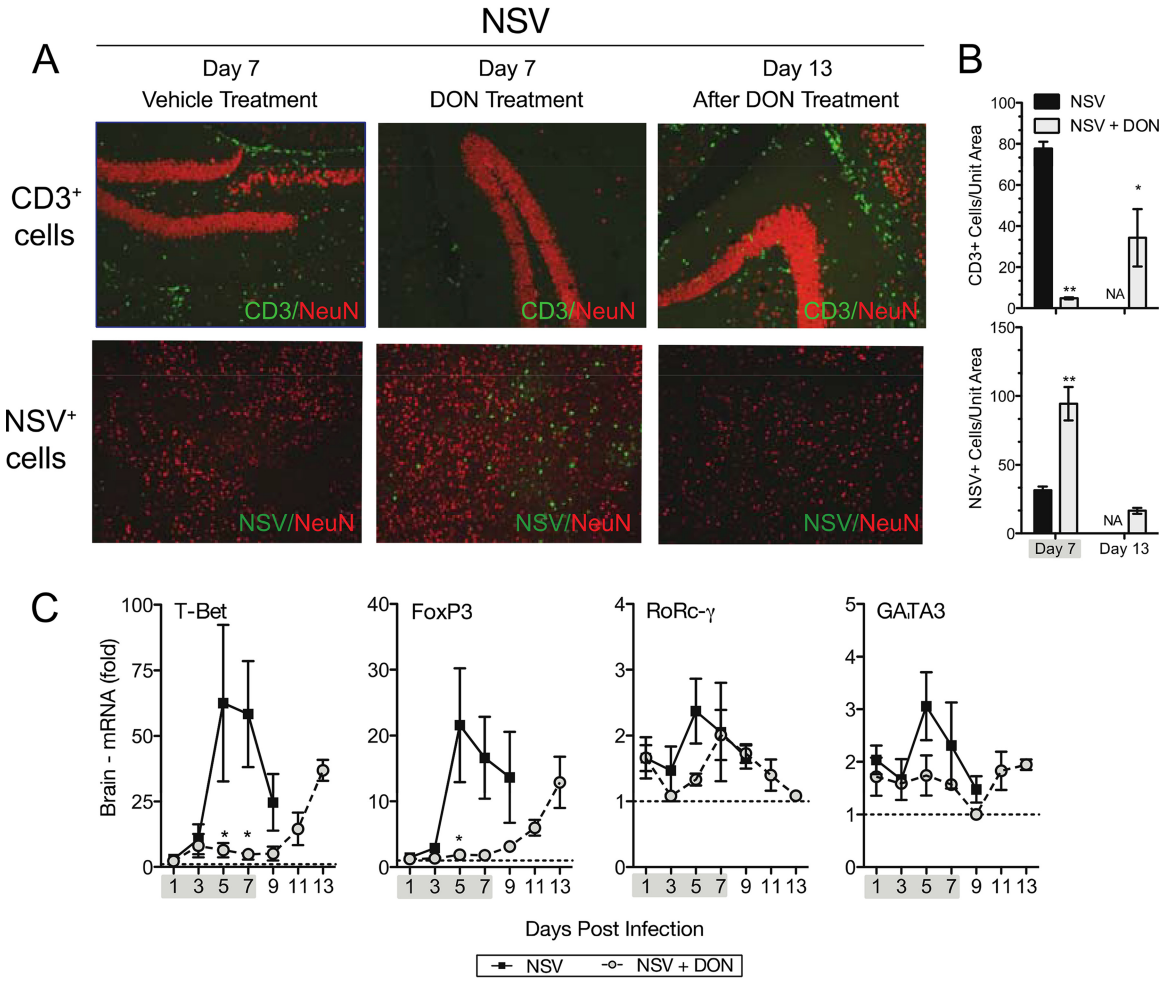

FIG 5 Changes in inflammation and viral antigen after DON treatment is halted. (A, top) Immunofluorescence of CD3-positive lymphocytes and the neuronal marker NeuN (red) in hippocampal brain sections at day 7 (treated and untreated) and day 13 (after treatment). (Bottom) Immunofluorescence of NSV antigen and NeuN in cortical brain sections at day 7 (treated and untreated) and day 13 (after treatment). (B) Quantification of $CD3^+$ cells (top) and NSV-infected cells (bottom). (C) Expression of T-cell-specific transcription factor mRNAs in the brain. Error bars represent standard errors of the means of data for three mice per time point per group (B and C). Mice were treated with 0.3 mg/kg (A and B) or 0.6 mg/kg (C) of DON or PBS once daily through day 7. Gray shading under the *x* axis identifies the drug treatment period. *, $P < 0.05$; **, $P < 0.01$; ***, $P < 0.001$ (as determined by one-way ANOVA [B] or two-way ANOVA with a Bonferroni posttest [C]).

absence of DON or ACI at 5 to 20 μM. Cells were stained for CD3, CD4 (PerCP-Cy 5.5, RM4-5 clone; BD Biosciences), and CD8 as described above. Viability was assessed at 12 h by flow cytometry (FACSCanto II; BD) using a violet fluorescent exclusion dye (Invitrogen) according to the manufacturer's protocol. T-cell proliferation was assessed at 72 h by CFSE dilution.

Enzyme immunoassays (EIAs). For the detection of NSV-specific IgG, 96-well plates were coated overnight at 4°C with lysates from BHK cells infected with NSV or uninfected BHK cells diluted in coating buffer (50 mM $NaHCO_3$, pH 9.6). Plates were washed with PBST, blocked with 10% FBS in PBST for 1 h at RT or overnight at 4°C, and washed. Mouse serum samples diluted 1:100 in blocking buffer were added and incubated for 1 h at RT. Plates were washed and incubated with horseradish peroxidase-conjugated anti-mouse IgG (1:2,000; Southern Biotech). Color was developed with TMB (3,3′,5,5′-tetramethylbenzidine) substrate solution (Sigma). After the addition of stop solution (2 M H_2SO_4), optical densities (ODs) at 450 nm were determined. OD values from wells coated with uninfected BHK lysates were subtracted to obtain NSV-specific OD values.

For measurement of IFN-γ and IL-2 levels, supernatant fluids collected from culture medium 24 h after the activation of $CD3^+$ splenocytes with anti-CD3 and -CD28 were assayed according to the manufacturer's instructions (R&D Systems). Clarified 20% brain homogenates diluted 1:2 were assayed for IFN-α, IFN-β (PBL Interferon Source), and IFN-γ (R&D Systems) according to the manufacturers' instructions.

Statistical analysis. Statistical analysis was performed by using Prism 5 software (GraphPad). Two-way analysis of variance (ANOVA) with a Bonferroni posttest was used for analysis of differences between treated and untreated mice at different time points. Student's *t* test was used to compare BrdU incorporation between groups. One-way ANOVA with Dunnett's posttest was used to compare BHK viral titers and *in vitro* T-cell responses. A log rank (Mantel-Cox) test was used to compare Kaplan-Meier survival curves. A *P* value of <0.05 was considered significant.

RESULTS

Glutamine antagonists protect mice from NSV-induced fatal paralysis. To determine whether DON could protect mice from NSV-induced fatal paralysis, infected mice were treated daily from the time of infection through 7 days after infection with either PBS

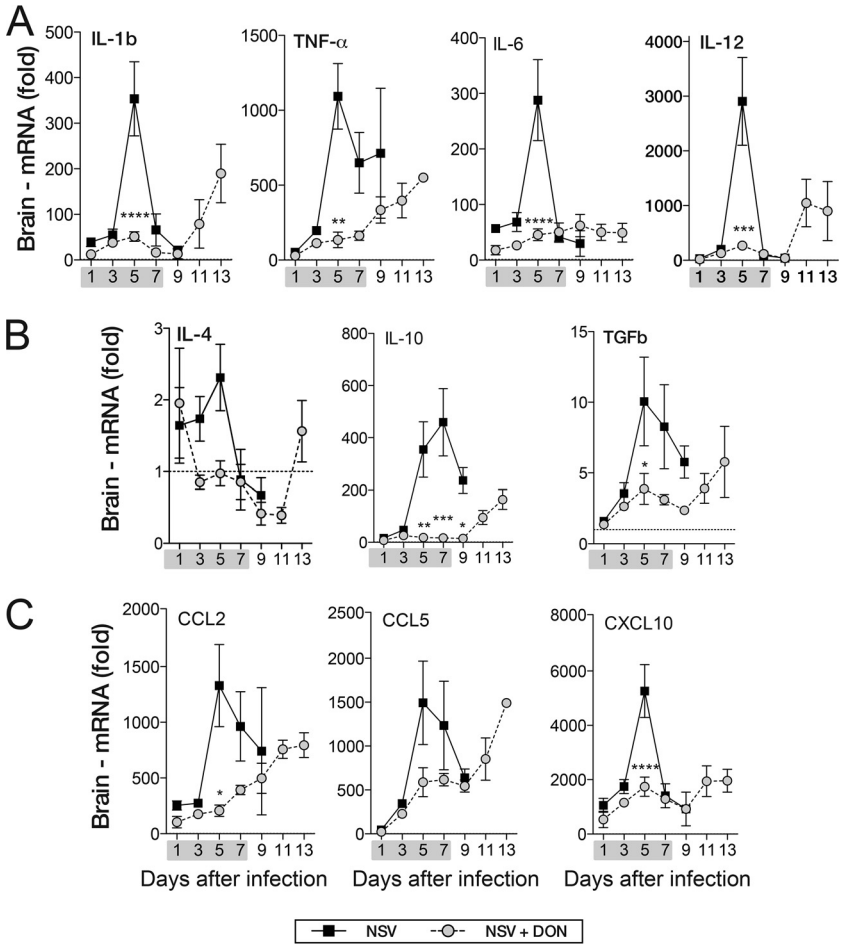

FIG 6 DON-treated mice have lower cytokine and chemokine mRNA levels in brain. Brains of DON-treated (NSV + DON) (0.6 mg/kg) and PBS-treated (NSV) mice were examined for levels of innate and adaptive cytokine and chemokine mRNAs by qRT-PCR. (A) mRNA levels of innate proinflammatory cytokines (IL-1β, TNF-α, IL-6, and IL-12). (B) mRNA levels of anti-inflammatory cytokines (IL-4, IL-10, and TGF-β). (C) mRNA levels of chemokines (CCL2, CCL5, and CXCL10). The gray bar under the *x* axis represents the drug treatment period (day 0 through day 7). Error bars represent standard errors of the means of data for three mice per time point. The dotted lines indicate the mRNA levels in uninfected mice. *, $P < 0.05$; **, $P < 0.01$; ***, $P < 0.001$; ****, $P < 0.0001$ (as determined by two-way ANOVA with a Bonferroni posttest).

or DON (0.3 mg/kg or 0.6 mg/kg) (Fig. 1). Most PBS-treated mice showed signs of paralysis by day 6 (Fig. 1A), and all mice died by day 12, with a median time to death of 8 days (Fig. 1B). During the period of treatment, DON-treated mice had lower clinical scores than did PBS-treated mice (Fig. 1A). However, once DON treatment was stopped, paralysis developed, and most mice died (Fig. 1B). Therefore, DON treatment delayed the onset of clinical disease, with median times to death of 14 days for the low dose (0.3 mg/kg) and 12 days for the high dose (0.6 mg/kg).

To determine whether another glutamine antagonist would have a similar effect, we also evaluated treatment with ACI, a nonspecific glutamine antagonist structurally distinct from DON. ACI was effective in preventing acute NSV-induced fatal paralysis in most mice during treatment (Fig. 1C) and also decreased mortality (Fig. 1D).

DON treatment has little effect on NSV replication or induction of IFN-α/β but delays virus clearance. To determine if glutamine deprivation or DON treatment affected NSV replication, virus growth in BHK cells was assessed (Fig. 2A). Cells were serum and glutamine starved for 24 h to deplete intracellular glutamine stores; infected with NSV at multiplicities of infection (MOIs) of 1 and 10; and cultured in either complete medium (DMEM, 1% dialyzed FBS, 2 mM glutamine, Pen-Strep), glutamine-deficient medium (DMEM without glutamine, 1% dialyzed FBS, Pen-Strep), or complete medium containing the glutamine antagonist DON or ACI (100 μM). Virus production was assessed at 24 h. Neither glutamine deprivation nor glutamine antagonists affected NSV replication *in vitro*.

To examine the effects of DON treatment on virus replication and clearance *in vivo*, brains and spinal cords were harvested and assayed for plaque formation. DON treatment had no effect on peak viral replication, with similar viral titers in the brains and spinal cords of treated and untreated mice (Fig. 2B). However, untreated mice showed decreasing viral titers on day 5 and clearance by day 7, while DON-treated mice did not clear the virus until days 11 to 13 after DON treatment was stopped. Clearance of the virus was associated with the onset of neurological disease in both DON-treated and PBS-treated mice (Fig. 1A).

To determine if DON treatment affected the induction of type I IFN, brain homogenates were assayed by EIAs for levels of IFN-α

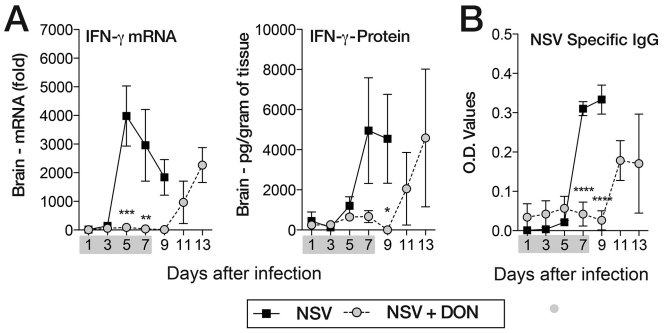

FIG 7 DON-treated mice have lower levels of IFN-γ mRNA and protein in the brain and lower levels of NSV-specific antibody in the serum during treatment. (A) Brain IFN-γ mRNA levels as measured by qRT-PCR and normalized to GAPDH and IFN-γ protein levels measured by enzyme-linked immunosorbent assays in brain homogenates from PBS-treated (NSV) and DON-treated (NSV + DON) (0.6 mg/kg) mice. (B) Levels of NSV-specific IgG in serum measured by EIA from DON-treated (NSV + DON) and PBS-treated (NSV) mice. The gray bar under the *x* axis identifies the treatment period (day 0 through day 7). Error bars represent standard errors of the means of data for three mice ($n = 3$ mice/day/group). *, $P < 0.05$; **, $P < 0.01$; ***, $P < 0.001$; ****, $P < 0.0001$ (as determined by two-way ANOVA with a Bonferroni post-test).

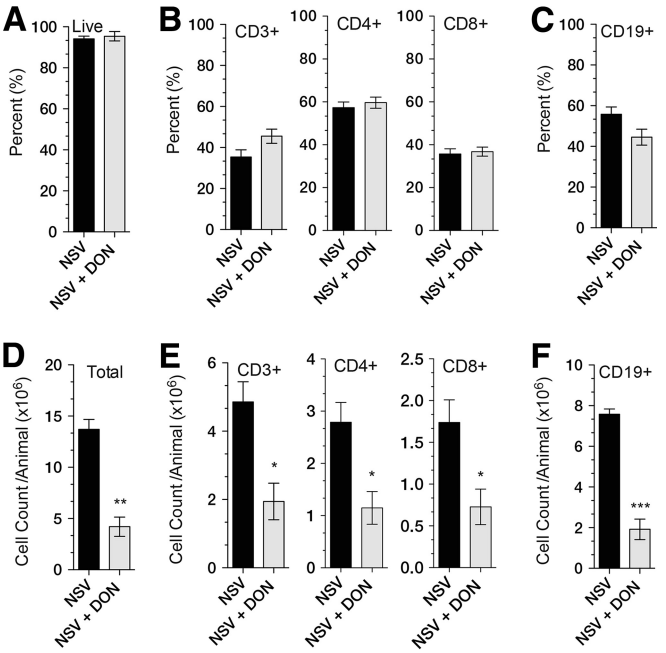

FIG 8 Effect of DON treatment on lymphocyte composition and counts in the draining superficial cervical lymph nodes. Superficial cervical lymph nodes from NSV-infected DON-treated (NSV + DON) and PBS-treated (NSV) mice were harvested on day 5, the peak time of lymphocyte proliferation in response to infection. (A to C) Proportions of total lymph node cells that are live (A); $CD3^+$, $CD4^+$, and $CD8^+$ (B); and $CD19^+$ (C). (D to F) Total numbers of live cells (D); $CD3^+$, $CD4^+$, and $CD8^+$ cells (E); and $CD19^+$ cells (F) per animal. Mice were treated with 0.3 mg/kg of DON or PBS once daily through day 7. Error bars represent standard errors of the means of data for three mice per time point per group *, $P < 0.05$; **, $P < 0.01$; ***, $P < 0.001$ (as determined by Student's *t* test).

and IFN-β (Fig. 2C). Similar levels of type I IFN were induced, although levels of IFN-α increased faster and levels of IFN-β decreased faster in DON-treated than in PBS-treated NSV-infected mice.

DON-treated mice have less CNS inflammation. Infiltrating leukocytes play a critical role in the clearance of NSV from the CNS but also contribute to neuronal damage (8, 10, 13). To determine the effects of DON treatment on leukocyte infiltration, we isolated and counted leukocytes in the brains of treated and untreated NSV-infected mice. During treatment, fewer leukocytes infiltrated the brains of DON-treated mice than untreated mice (Fig. 3). Total leukocyte counts ($CD45^+$) and T-lymphocyte ($CD3^+$) counts, as well as $CD4^+$ and $CD8^+$ T-cell and $CD19^+$ B-cell counts, were higher in untreated mice 5 and 7 days after infection.

Analysis of H&E-stained brain and spinal cord sections showed less inflammation in DON-treated mice than in PBS-treated mice on day 7 (Fig. 4). However, mononuclear cells infiltrated the brains and spinal cords of surviving DON-treated mice on day 13, 6 days after the cessation of DON treatment. A similar trend was seen with infiltrating $CD3^+$ lymphocytes when assessed by immunofluorescence staining (Fig. 5A and B, top), with few cells in the brains of DON-treated mice on day 7 but many cells on day 13. Cellular infiltration was coincident with clearance of the virus, as indicated by the detection of NSV antigen by immunofluorescence staining (Fig. 5A and B, bottom) and of infectious virus by plaque assays (Fig. 2B).

qRT-PCR for mRNAs of the T-cell-subtype-specific transcription factors T-bet (Th1), FoxP3 (Treg), RoRc-γ (Th17), and GATA3 (Th2) showed that all subsets were affected by DON treatment, with the most marked effect being seen on T-bet- and FoxP3-expressing cells (Fig. 5C).

DON-treated mice have lower levels of cytokine and chemokine mRNAs in brain. To investigate the effects of DON treatment on inflammatory mediators in the CNS, brains from DON-treated and PBS-treated NSV-infected mice were assayed for proinflammatory cytokine (IL-1β, IL-6, TNF-α, and IL-12), anti-inflammatory cytokine (IL-10, TGF-β, and IL-4), and chemokine (CCL2, CCL5, and CXCL10) mRNAs (Fig. 6). PBS-treated mice had peak proinflammatory mRNA expression at day 5 (Fig. 6A). IL-1β, IL-6, and IL-12 mRNA levels decreased to day 1 levels by day 7, while TNF-α mRNA levels remained high for a longer period (Fig. 6A). Proinflammatory cytokine mRNA levels did not increase during DON treatment but, with the exception of IL-6, increased 9 to 11 days after infection, when treatment had been stopped (Fig. 6A). The brains of DON-treated mice also had lower levels of anti-inflammatory cytokine (Fig. 6B) and chemokine (Fig. 6C) mRNAs during treatment that increased after DON treatment was stopped.

DON-treated mice have lower levels of IFN-γ in brain and NSV-specific antibody in serum. Previous studies have shown that IFN-γ and antibody to the E2 glycoprotein are the main effectors of clearance of infectious virus from the brain and spinal cord through noncytolytic mechanisms (33–36). Because clearance is delayed in DON-treated mice, we measured the effect of treatment on IFN-γ mRNA and protein levels in the brain and on NSV-specific antibody in serum (Fig. 7). In untreated NSV-infected mice, IFN-γ mRNA levels peaked on day 5 after infection, and IFN-γ protein levels peaked soon after, on day 7. In DON-treated mice, neither IFN-γ mRNA nor protein levels increased during treatment, but levels increased on days 11 and 13 after DON was discontinued (Fig. 7A). Similarly, NSV-specific IgG was

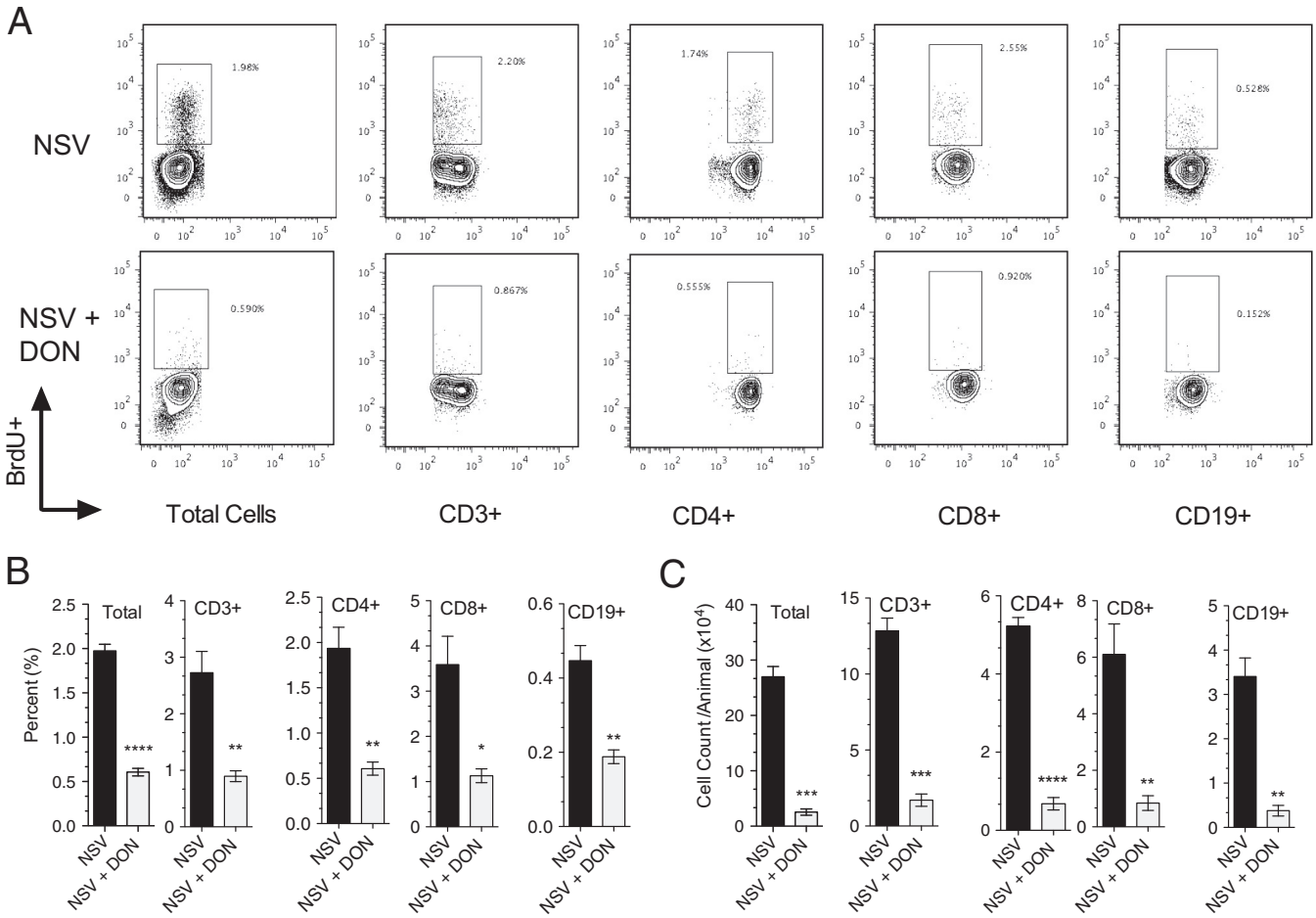

FIG 9 Effect of DON on lymphocyte proliferation during NSV infection. Mice were pulsed with BrdU to label proliferating cells on days 4 and 5 after infection. Cells were collected 8 h later, and BrdU incorporation was measured by flow cytometry. The percentages (A and B) and absolute numbers (C) of total cells and $CD3^+$, $CD4^+$, $CD8^+$, and $CD19^+$ lymphocytes incorporating BrdU were determined. Mice were treated with DON (0.3 mg/kg) or PBS from day 0 through day 7. Error bars represent standard errors of the means of data for three mice per time point per group (B and C). Data are representative of results from two independent experiments. *, $P < 0.05$; **, $P < 0.01$; ***, $P < 0.001$; ****, $P < 0.0001$ (as determined by Student's *t* test).

present in serum of untreated mice on days 7 to 9 after infection, but mice treated with DON produced little antibody until days 11 to 13 (Fig. 7B). The appearance of IFN-γ in brain and antibody in serum was coincident with the clearance of infectious virus in both PBS-treated and DON-treated mice (Fig. 2B).

Levels of lymphocyte proliferation in the draining cervical lymph nodes after infection are lower in DON-treated than in PBS-treated mice. The induction of the adaptive immune response to NSV infection of the brain occurs primarily in the superficial and deep cervical lymph nodes, and lymphocyte proliferation peaks 5 days after infection. To determine the effects of DON on the induction of lymphoid cell responses to infection, superficial cervical lymph nodes were isolated from PBS-treated and DON-treated NSV-infected mice at day 5. Cells were stained for CD45, CD3, CD4, CD8, and CD19 and counted by flow cytometry (Fig. 8). The percentages of viable cells were similar (Fig. 8A), as were the proportions of CD3-, CD4-, CD8-, and CD19-positive cells (Fig. 8B and C). However, there were fewer lymphocytes for all subsets in DON-treated mice, likely indicating a failure to proliferate in response to infection (Fig. 8D to F).

To directly assess the proliferation of cells in the draining lymph nodes, mice were pulsed with the thymidine analogue BrdU 4 and 5 days after infection. Proliferating cells incorporate BrdU during the S phase of the cell cycle, and BrdU positivity identifies cells that are proliferating during the labeling period. Lymph nodes were harvested 8 h after the second dose on day 5, and cells were assessed for BrdU incorporation via flow cytometry (Fig. 9A). DON-treated mice had a lower percentage (Fig. 9B) and number (Fig. 9C) of BrdU-positive T cells and B cells than did PBS-treated mice, indicating reduced proliferation after infection in the presence of DON.

DON inhibits T-cell proliferation *in vitro*. Because the *in vivo* data indicate a failure of lymphocyte proliferation in response to NSV infection, we sought to directly test the effect of glutamine antagonism on the response of T lymphocytes to nonspecific stimulation through the T-cell receptor (TCR) *in vitro*. Purified primary splenic T cells were stimulated with anti-CD3/anti-CD28, and growth and proliferation were measured in the presence of DON and ACI and in the absence of glutamine (Fig. 10). Treatment with the glutamine antagonist DON or ACI did not affect cell viability, but treated cells failed to proliferate in response to stimulation. CFSE dilution profiles showed that, like glutamine-

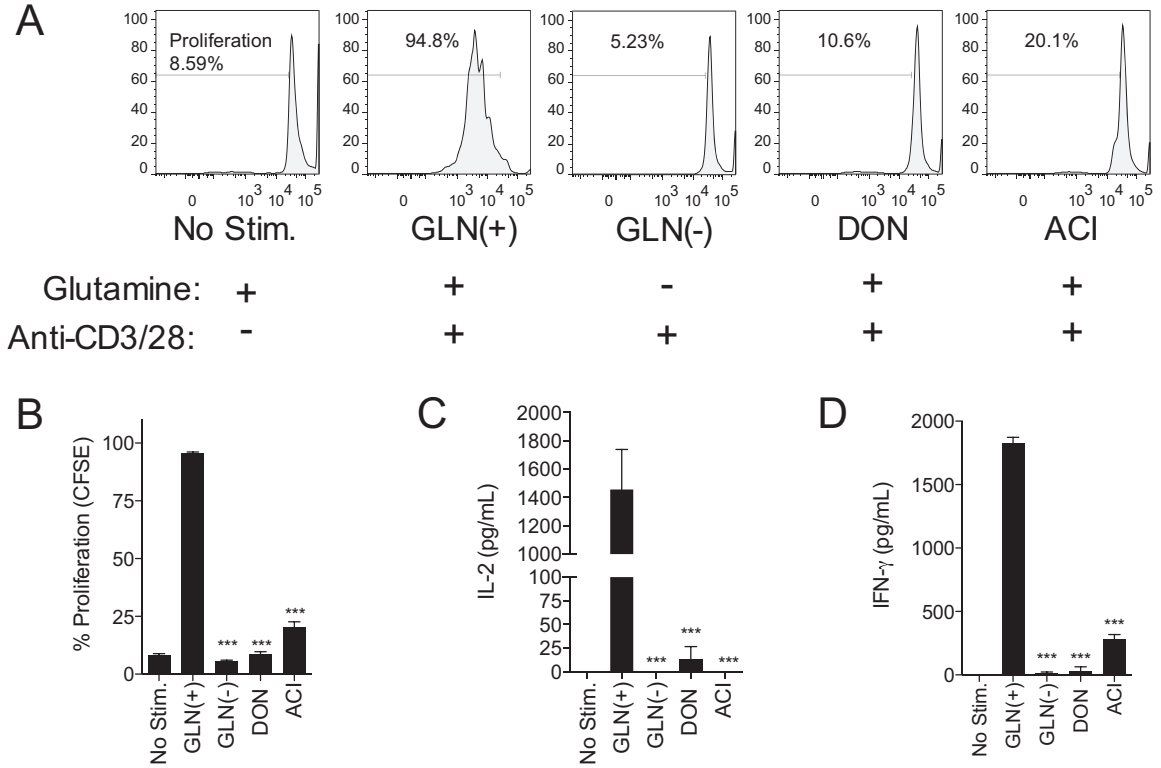

FIG 10 Glutamine antagonists inhibit T-cell proliferation *in vitro*. Spleen CD3$^+$ T cells were stimulated with anti-CD3/anti-CD28. Stimulated cells were either supplemented with glutamine [Gln(+)], deprived of glutamine [Gln(−)], or treated with glutamine antagonists (DON and ACI) in glutamine-supplemented medium. (A) CFSE proliferation assay of stimulated T cells after 72 h. (B) Quantitation of CFSE data. (C and D) Enzyme-linked immunosorbent assays of the T-cell growth factors IL-2 (C) and IFN-γ (D). Error bars represent standard errors of the means for three biological replicates. Data are representative of the results of at least two independent experiments. ***, $P < 0.001$ (as determined by one-way ANOVA with Dunnett's posttest).

deprived lymphocytes, DON- and ACI-treated lymphocytes failed to undergo even one round of division after stimulation (Fig. 10A). The profiles of DON- and ACI-treated stimulated lymphocytes were similar to those of glutamine-deprived stimulated lymphocytes and unstimulated lymphocytes (Fig. 10A and B). Because the production of IL-2 is essential for lymphocyte growth in response to stimulation, the level of IL-2 was measured. DON- and ACI-treated lymphocytes as well as glutamine-deprived lymphocytes did not produce IL-2 (Fig. 10C) or IFN-γ (Fig. 10D) in response to stimulation.

DISCUSSION

Treatment of mice for 7 days with the glutamine antagonist DON delayed the onset of NSV-induced acute fatal paralysis. DON prevented the induction of the antiviral immune response, resulting in decreased CNS inflammation and a failure to clear infectious virus from the brain and spinal cord. Analysis of draining cervical lymph node cells showed that proliferation of B cells and CD4$^+$ and CD8$^+$ T cells in response to infection was prevented by DON treatment. Mice that survived acute infection as a result of treatment succumbed to NSV-induced fatal encephalomyelitis after treatment was stopped, coincident with the appearance of the antiviral immune response, increased CNS inflammation, and virus clearance.

Research going back to the 1970s and 1980s has shown that glutamine deprivation affects lymphocyte proliferation (37–40), but glutamine antagonists have received little study for immune modulation of immunopathological diseases. Due to an increased understanding of how fundamental metabolites such as glutamine can affect the immune response, recent attention has been focused in this area (15, 41–44). Rapidly proliferating lymphocytes preferentially utilize glutamine over glucose to satisfy their metabolic needs, making glutamine metabolism a bottleneck that can be pharmacologically exploited for immunomodulation (41, 45).

Treatment with DON prevented the growth and proliferation of peripheral lymphocytes involved in the antiviral immune response, leading to decreased CNS lymphocyte infiltration and delayed viral clearance. The production of IFN-γ and NSV-specific IgG, both of which are important for virus clearance, was compromised in DON-treated mice. A role for the antiviral immune response in disease is empirically supported by the appearance of proinflammatory, chemotactic, anti-inflammatory, and T-cell transcription factor mRNAs in the brain after DON treatment was stopped. Previous studies have shown that susceptible C57BL/6 mice deficient in TCR-alpha and -beta, class I antigen presentation (β2 microglobulin and TAP1), or CD4$^+$ T cells have improved survival after NSV infection and that IL-10-deficient mice have accelerated disease, suggesting a prominent role for T cells in NSV-induced disease (7, 8, 13). Furthermore, the depletion of neither circulating monocytes nor neutrophils alters the course of NSV-induced fatal disease (13, 46).

These data suggest that T cells are the primary mediators of

neuronal death in NSV-induced acute encephalomyelitis. How T cells mediate disease is still unknown, and prevention of disease development by DON may be through more than one mechanism. Neurotropic infections of the CNS can lead to glutamate excitotoxicity through both direct neuronal damage and immune-mediated neuronal injury (11, 12, 47–49). Cultured primary cortical and spinal cord neurons infected with NSV develop direct and bystander neuronal death that can be ameliorated by using antagonists of the NMDA and AMPA ionotropic glutamate receptors (50, 51). In NSV-infected mice, treatment with *N*-methyl-D-aspartate (NMDA) and AMPA receptor antagonists protects hippocampal neurons against neurodegeneration, but only AMPA receptor antagonists protect spinal cord motor neurons and prevent NSV-induced fatal paralysis (11, 12). Surprisingly, mice treated with AMPA receptor antagonists showed delayed viral clearance, a decreased peripheral immune response, and less CNS inflammation. Therefore, treatment with DON produced an outcome similar to that of treatment with AMPA receptor antagonists through a very different mechanism.

DON may prevent the generation of neurotoxic glutamate as well as inhibit the growth and proliferation of lymphocytes in peripheral lymphoid tissue. DON is effective in preventing the generation of glutamate by microglial cells and macrophages, and mitigation of disease in experimental autoimmune encephalomyelitis is assumed to be due to the prevention of glutamate release (52). Viral infections can increase glutamate production by microglia (53, 54) and infiltration of activated $CD8^+$ T cells that can be a potent source of nonneuronal glutamate (55). Inhibition of glutamine metabolism may prevent the generation of glutamate and reduce excitotoxic damage to neurons (53, 54, 56). However, our study was not able to address the relative contribution of excitotoxic damage to fatal disease but was able to show that DON has potent inhibitory effects on the induction of the immune response that correlated with disease.

Glutamine deprivation and treatment with drugs that inhibit glutamine metabolism could also have a direct effect on virus replication (57–63) and were previously reported to reduce titers of SINV produced by BHK cells (63). However, we were unable to replicate these effects either *in vitro* or *in vivo*, as neither glutamine deprivation nor DON treatment affected NSV replication in our studies.

DON is a relatively nonspecific inhibitor of all glutamine-utilizing enzymes; high doses have been associated with substantial toxicity, and in mice, DON alone for a week results in some weight loss but no mortality (25, 26, 30). Although short-term treatment was relatively well tolerated, more specific inhibitors may facilitate more prolonged treatment. GLS1 is the major glutaminase involved in the generation of glutamate in the CNS (64) and has a central role in glutamine metabolism, cell cycle progression, and signaling in rapidly proliferating cells, including activated lymphocytes (16, 18, 28, 45, 65–67). Therefore, the use of GLS1-specific inhibitors might offer a more specific, targeted, and less toxic way to treat neuroinflammatory disease. Modulation of the induction of virus-specific lymphocyte responses may provide a promising approach for the treatment of viral encephalomyelitis, particularly if used in combination with a drug that can inhibit virus replication.

ACKNOWLEDGMENTS

This work was supported in part by research and training grants R01 NS087539 (D.E.G.), T32 OD011089 (V.K.B.), T32 AI007247 (K.L.W.S.), and T32 AI007417 (S.M.) from the National Institutes of Health and a pilot grant from the Johns Hopkins Brain Science Institute (D.E.G.).

We thank Jonathan Powell and Kirsten Kulcsar for helpful advice on this project.

FUNDING INFORMATION

This work, including the efforts of Barbara S. Slusher, was funded by Johns Hopkins Brain Science Institute (pilot grant). This work, including the efforts of Diane E. Griffin, was funded by HHS | National Institutes of Health (NIH) (R01 NS087539, T32 OD011089, T32 AI007247, and T32 AI 07417).

REFERENCES

1. **Adouchief S, Smura T, Sane J, Vapalahti O, Kurkela S.** 15 March 2016. Sindbis virus as a human pathogen—epidemiology, clinical picture and pathogenesis. Rev Med Virol http://dx.doi.org/10.1002/rmv.1876.
2. **Jackson AC, Moench TR, Griffin DE, Johnson RT.** 1987. The pathogenesis of spinal cord involvement in the encephalomyelitis of mice caused by neuroadapted Sindbis virus infection. Lab Invest **56:**418–423.
3. **Thach DC, Kimura T, Griffin DE.** 2000. Differences between C57BL/6 and BALB/cBy mice in mortality and virus replication after intranasal infection with neuroadapted Sindbis virus. J Virol **74:**6156–6161. http://dx.doi.org/10.1128/JVI.74.13.6156-6161.2000.
4. **Tucker PC, Griffin DE.** 1991. Mechanism of altered Sindbis virus neurovirulence associated with a single-amino-acid change in the E2 glycoprotein. J Virol **65:**1551–1557.
5. **Johnson RT, McFarland HF, Levy SE.** 1972. Age-dependent resistance to viral encephalitis: studies of infections due to Sindbis virus in mice. J Infect Dis **125:**257–262. http://dx.doi.org/10.1093/infdis/125.3.257.
6. **Tucker PC, Griffin DE, Choi S, Bui N, Wesselingh S.** 1996. Inhibition of nitric oxide synthesis increases mortality in Sindbis virus encephalitis. J Virol **70:**3972–3977.
7. **Rowell JF, Griffin DE.** 2002. Contribution of T cells to mortality in neurovirulent Sindbis virus encephalomyelitis. J Neuroimmunol **127:**106–114. http://dx.doi.org/10.1016/S0165-5728(02)00108-X.
8. **Kimura T, Griffin DE.** 2000. The role of CD8(+) T cells and major histocompatibility complex class I expression in the central nervous system of mice infected with neurovirulent Sindbis virus. J Virol **74:**6117–6125. http://dx.doi.org/10.1128/JVI.74.13.6117-6125.2000.
9. **Griffin DE, Johnson RT.** 1977. Role of the immune response in recovery from Sindbis virus encephalitis in mice. J Immunol **118:**1070–1075.
10. **Kimura T, Griffin DE.** 2003. Extensive immune-mediated hippocampal damage in mice surviving infection with neuroadapted Sindbis virus. Virology **311:**28–39. http://dx.doi.org/10.1016/S0042-6822(03)00110-7.
11. **Greene IP, Lee EY, Prow N, Ngwang B, Griffin DE.** 2008. Protection from fatal viral encephalomyelitis: AMPA receptor antagonists have a direct effect on the inflammatory response to infection. Proc Natl Acad Sci U S A **105:**3575–3580. http://dx.doi.org/10.1073/pnas.0712390105.
12. **Nargi-Aizenman JL, Havert MB, Zhang M, Irani DN, Rothstein JD, Griffin DE.** 2004. Glutamate receptor antagonists protect from virus-induced neural degeneration. Ann Neurol **55:**541–549. http://dx.doi.org/10.1002/ana.20033.
13. **Kulcsar KA, Baxter VK, Greene IP, Griffin DE.** 2014. Interleukin 10 modulation of pathogenic Th17 cells during fatal alphavirus encephalomyelitis. Proc Natl Acad Sci U S A **111:**16053–16058. http://dx.doi.org/10.1073/pnas.1418966111.
14. **MacIver NJ, Michalek RD, Rathmell JC.** 2013. Metabolic regulation of T lymphocytes. Annu Rev Immunol **31:**259–283. http://dx.doi.org/10.1146/annurev-immunol-032712-095956.
15. **Maciolek JA, Pasternak JA, Wilson HL.** 2014. Metabolism of activated T lymphocytes. Curr Opin Immunol **27:**60–74. http://dx.doi.org/10.1016/j.coi.2014.01.006.
16. **Carr EL, Kelman A, Wu GS, Gopaul R, Senkevitch E, Aghvanyan A, Turay AM, Frauwirth KA.** 2010. Glutamine uptake and metabolism are coordinately regulated by ERK/MAPK during T lymphocyte activation. J Immunol **185:**1037–1044. http://dx.doi.org/10.4049/jimmunol.0903586.
17. **Pollizzi KN, Powell JD.** 2014. Integrating canonical and metabolic sig-

nalling programmes in the regulation of T cell responses. Nat Rev Immunol **14:**435–446. http://dx.doi.org/10.1038/nri3701.
18. **Colombo SL, Palacios-Callender M, Frakich N, De Leon J, Schmitt CA, Boorn L, Davis N, Moncada S.** 2010. Anaphase-promoting complex/cyclosome-Cdh1 coordinates glycolysis and glutaminolysis with transition to S phase in human T lymphocytes. Proc Natl Acad Sci U S A **107:** 18868–18873. http://dx.doi.org/10.1073/pnas.1012362107.
19. **Meldrum B, Garthwaite J.** 1990. Excitatory amino acid neurotoxicity and neurodegenerative disease. Trends Pharmacol Sci **11:**379–387. http://dx.doi.org/10.1016/0165-6147(90)90184-A.
20. **Choi DW.** 1988. Glutamate neurotoxicity and diseases of the nervous system. Neuron **1:**623–634. http://dx.doi.org/10.1016/0896-6273(88)90162-6.
21. **Thangavelu K, Chong QY, Low BC, Sivaraman J.** 2014. Structural basis for the active site inhibition mechanism of human kidney-type glutaminase (KGA). Sci Rep **4:**3827. http://dx.doi.org/10.1038/srep03827.
22. **Coffey GL, Ehrlich J, Fisher MW, Hillegas AB, Kohberger DL, Machamer HE, Rightsel WA, Roegner FR.** 1956. 6-Diazo-5-oxo-L-norleucine, a new tumor-inhibitory substance. I. Biologic studies. Antibiot Chemother (Northfield) **6:**487–497.
23. **Kisner DL, Catane R, Muggia FM.** 1980. The rediscovery of DON (6-diazo-5-oxo-L-norleucine). Recent Results Cancer Res **74:**258–263. http://dx.doi.org/10.1007/978-3-642-81488-4_30.
24. **Lynch G, Kemeny N, Casper E.** 1982. Phase II evaluation of DON (6-diazo-5-oxo-L-norleucine) in patients with advanced colorectal carcinoma. Am J Clin Oncol **5:**541–543. http://dx.doi.org/10.1097/00000421-198210000-00014.
25. **Earhart RH, Koeller JM, Davis HL.** 1982. Phase I trial of 6-diazo-5-oxo-L-norleucine (DON) administered by 5-day courses. Cancer Treat Rep **66:**1215–1217.
26. **Sullivan MP, Nelson JA, Feldman S, Van Nguyen B.** 1988. Pharmacokinetic and phase I study of intravenous DON (6-diazo-5-oxo-L-norleucine) in children. Cancer Chemother Pharmacol **21:**78–84. http://dx.doi.org/10.1007/BF00262746.
27. **Earhart RH, Amato DJ, Chang AY, Borden EC, Shiraki M, Dowd ME, Comis RL, Davis TE, Smith TJ.** 1990. Phase II trial of 6-diazo-5-oxo-L-norleucine versus aclacinomycin-A in advanced sarcomas and mesotheliomas. Invest New Drugs **8:**113–119.
28. **Wang R, Dillon CP, Shi LZ, Milasta S, Carter R, Finkelstein D, McCormick LL, Fitzgerald P, Chi H, Munger J, Green DR.** 2011. The transcription factor Myc controls metabolic reprogramming upon T lymphocyte activation. Immunity **35:**871–882. http://dx.doi.org/10.1016/j.immuni.2011.09.021.
29. **Lee CF, Lo YC, Cheng CH, Furtmuller GJ, Oh B, Andrade-Oliveira V, Thomas AG, Bowman CE, Slusher BS, Wolfgang MJ, Brandacher G, Powell JD.** 2015. Preventing allograft rejection by targeting immune metabolism. Cell Rep **13:**760–770. http://dx.doi.org/10.1016/j.celrep.2015.09.036.
30. **Potter MC, Baxter VK, Mathey RW, Alt J, Rojas C, Griffin DE, Slusher BS.** 2015. Neurological sequelae induced by alphavirus infection of the CNS are attenuated by treatment with the glutamine antagonist 6-diazo-5-oxo-L-norleucine. J Neurovirol **21:**159–173. http://dx.doi.org/10.1007/s13365-015-0314-6.
31. **Gordon EB, Hart GT, Tran TM, Waisberg M, Akkaya M, Kim AS, Hamilton SE, Pena M, Yazew T, Qi CF, Lee CF, Lo YC, Miller LH, Powell JD, Pierce SK.** 2015. Targeting glutamine metabolism rescues mice from late-stage cerebral malaria. Proc Natl Acad Sci U S A **112:** 13075–13080. http://dx.doi.org/10.1073/pnas.1516544112.
32. **Pino PA, Cardona AE.** 2 February 2011. Isolation of brain and spinal cord mononuclear cells using Percoll gradients. J Vis Exp http://dx.doi.org/10.3791/2348.
33. **Binder GK, Griffin DE.** 2001. Interferon-gamma-mediated site-specific clearance of alphavirus from CNS neurons. Science **293:**303–306. http://dx.doi.org/10.1126/science.1059742.
34. **Burdeinick-Kerr R, Griffin DE.** 2005. Gamma interferon-dependent, noncytolytic clearance of Sindbis virus infection from neurons in vitro. J Virol **79:**5374–5385. http://dx.doi.org/10.1128/JVI.79.9.5374-5385.2005.
35. **Levine B, Hardwick JM, Trapp BD, Crawford TO, Bollinger RC, Griffin DE.** 1991. Antibody-mediated clearance of alphavirus infection from neurons. Science **254:**856–860. http://dx.doi.org/10.1126/science.1658936.
36. **Burdeinick-Kerr R, Govindarajan D, Griffin DE.** 2009. Noncytolytic clearance of Sindbis virus infection from neurons by gamma interferon is dependent on Jak/STAT signaling. J Virol **83:**3429–3435. http://dx.doi.org/10.1128/JVI.02381-08.
37. **Hersh EM.** 1971. L-Glutaminase: suppression of lymphocyte blastogenic responses in vitro. Science **172:**736–738. http://dx.doi.org/10.1126/science.172.3984.736.
38. **Ardawi MS, Newsholme EA.** 1983. Glutamine metabolism in lymphocytes of the rat. Biochem J **212:**835–842. http://dx.doi.org/10.1042/bj2120835.
39. **Ardawi MS.** 1988. Glutamine and glucose metabolism in human peripheral lymphocytes. Metabolism **37:**99–103. http://dx.doi.org/10.1016/0026-0495(88)90036-4.
40. **Kafkewitz D, Bendich A.** 1983. Enzyme-induced asparagine and glutamine depletion and immune system function. Am J Clin Nutr **37:**1025–1030.
41. **Liu H, Yang H, Chen X, Lu Y, Zhang Z, Wang J, Zhang M, Xue L, Xue F, Liu G.** 19 May 2014. Cellular metabolism modulation in T lymphocyte immunity. Immunology http://dx.doi.org/10.1111/imm.12321.
42. **Altman BJ, Dang CV.** 2012. Normal and cancer cell metabolism: lymphocytes and lymphoma. FEBS J **279:**2598–2609. http://dx.doi.org/10.1111/j.1742-4658.2012.08651.x.
43. **Rathmell JC.** 2011. T cell Myc-tabolism. Immunity **35:**845–846. http://dx.doi.org/10.1016/j.immuni.2011.12.001.
44. **Poffenberger MC, Jones RG.** 2014. Amino acids fuel T cell-mediated inflammation. Immunity **40:**635–637. http://dx.doi.org/10.1016/j.immuni.2014.04.017.
45. **Le A, Lane AN, Hamaker M, Bose S, Gouw A, Barbi J, Tsukamoto T, Rojas CJ, Slusher BS, Zhang H, Zimmerman LJ, Liebler DC, Slebos RJ, Lorkiewicz PK, Higashi RM, Fan TW, Dang CV.** 2012. Glucose-independent glutamine metabolism via TCA cycling for proliferation and survival in B cells. Cell Metab **15:**110–121. http://dx.doi.org/10.1016/j.cmet.2011.12.009.
46. **Esen N, Blakely PK, Rainey-Barger EK, Irani DN.** 2012. Complexity of the microglial activation pathways that drive innate host responses during lethal alphavirus encephalitis in mice. ASN Neuro **4:**207–221. http://dx.doi.org/10.1042/AN20120016.
47. **Brison E, Jacomy H, Desforges M, Talbot PJ.** 2014. Novel treatment with neuroprotective and antiviral properties against a neuroinvasive human respiratory virus. J Virol **88:**1548–1563. http://dx.doi.org/10.1128/JVI.02972-13.
48. **Brison E, Jacomy H, Desforges M, Talbot PJ.** 2011. Glutamate excitotoxicity is involved in the induction of paralysis in mice after infection by a human coronavirus with a single point mutation in its spike protein. J Virol **85:**12464–12473. http://dx.doi.org/10.1128/JVI.05576-11.
49. **Blakely PK, Kleinschmidt-DeMasters BK, Tyler KL, Irani DN.** 2009. Disrupted glutamate transporter expression in the spinal cord with acute flaccid paralysis caused by West Nile virus infection. J Neuropathol Exp Neurol **68:** 1061–1072. http://dx.doi.org/10.1097/NEN.0b013e3181b8ba14.
50. **Darman J, Backovic S, Dike S, Maragakis NJ, Krishnan C, Rothstein JD, Irani DN, Kerr DA.** 2004. Viral-induced spinal motor neuron death is non-cell-autonomous and involves glutamate excitotoxicity. J Neurosci **24:**7566–7575. http://dx.doi.org/10.1523/JNEUROSCI.2002-04.2004.
51. **Nargi-Aizenman JL, Griffin DE.** 2001. Sindbis virus-induced neuronal death is both necrotic and apoptotic and is ameliorated by *N*-methyl-D-aspartate receptor antagonists. J Virol **75:**7114–7121. http://dx.doi.org/10.1128/JVI.75.15.7114-7121.2001.
52. **Shijie J, Takeuchi H, Yawata I, Harada Y, Sonobe Y, Doi Y, Liang J, Hua L, Yasuoka S, Zhou Y, Noda M, Kawanokuchi J, Mizuno T, Suzumura A.** 2009. Blockade of glutamate release from microglia attenuates experimental autoimmune encephalomyelitis in mice. Tohoku J Exp Med **217:** 87–92. http://dx.doi.org/10.1620/tjem.217.87.
53. **Chen CJ, Ou YC, Chang CY, Pan HC, Liao SL, Chen SY, Raung SL, Lai CY.** 2012. Glutamate released by Japanese encephalitis virus-infected microglia involves TNF-alpha signaling and contributes to neuronal death. Glia **60:**487–501. http://dx.doi.org/10.1002/glia.22282.
54. **Huang Y, Zhao L, Jia B, Wu L, Li Y, Curthoys N, Zheng JC.** 2011. Glutaminase dysregulation in HIV-1-infected human microglia mediates neurotoxicity: relevant to HIV-1-associated neurocognitive disorders. J Neurosci **31:**15195–15204. http://dx.doi.org/10.1523/JNEUROSCI.2051-11.2011.
55. **Melzer N, Hicking G, Bittner S, Bobak N, Gobel K, Herrmann AM, Wiendl H, Meuth SG.** 2013. Excitotoxic neuronal cell death during an oligodendrocyte-directed CD8+ T cell attack in the CNS gray matter. J Neuroinflammation **10:**121. http://dx.doi.org/10.1186/1742-2094-10-121.
56. **Zhao L, Huang Y, Tian C, Taylor L, Curthoys N, Wang Y, Vernon H, Zheng J.** 2012. Interferon-alpha regulates glutaminase 1 promoter

through STAT1 phosphorylation: relevance to HIV-1 associated neurocognitive disorders. PLoS One **7:**e32995. http://dx.doi.org/10.1371/journal.pone.0032995.

57. **Fontaine KA, Camarda R, Lagunoff M.** 2014. Vaccinia virus requires glutamine but not glucose for efficient replication. J Virol **88:**4366–4374. http://dx.doi.org/10.1128/JVI.03134-13.
58. **Cinatl J, Vogel JU, Cinatl J, Kabickova H, Kornhuber B, Doerr HW.** 1997. Antiviral effects of 6-diazo-5-oxo-L-norleucin on replication of herpes simplex virus type 1. Antiviral Res **33:**165–175. http://dx.doi.org/10.1016/S0166-3542(96)01012-1.
59. **Huang RC, Panin M, Romito RR, Huang YT.** 1994. Inhibition of replication of human respiratory syncytial virus by 6-diazo-5-oxo-L-norleucine. Antiviral Res **25:**269–279. http://dx.doi.org/10.1016/0166-3542(94)90009-4.
60. **Roberts J, McGregor WG.** 1991. Inhibition of mouse retroviral disease by bioactive glutaminase-asparaginase. J Gen Virol **72**(Part 2)**:**299–305.
61. **Nishio M, Tsurudome M, Bando H, Komada H, Ito Y.** 1990. Antiviral effect of 6-diazo-5-oxo-L-norleucine, antagonist of gamma-glutamyl transpeptidase, on replication of human parainfluenza virus type 2. J Gen Virol **71**(Part 1)**:**61–67.
62. **Goldstein G, Guskey LE.** 1984. Poliovirus and vesicular stomatitis virus replication in the presence of 6-diazo-5-oxo-L-norleucine or 2-deoxy-D-glucose. J Med Virol **14:**159–167. http://dx.doi.org/10.1002/jmv.1890140210.
63. **Ito Y, Kimura Y, Nagata I, Kunii A.** 1974. Effects of L-glutamine deprivation on growth of HVJ (Sendai virus) in BHK cells. J Virol **13:**557–566.
64. **El Hage M, Masson J, Conjard-Duplany A, Ferrier B, Baverel G, Martin G.** 2012. Brain slices from glutaminase-deficient mice metabolize less glutamine: a cellular metabolomic study with carbon 13 NMR. J Cereb Blood Flow Metab **32:**816–824. http://dx.doi.org/10.1038/jcbfm.2012.22.
65. **Glick GD, Rossignol R, Lyssiotis CA, Wahl D, Lesch C, Sanchez B, Liu X, Hao LY, Taylor C, Hurd A, Ferrara JL, Tkachev V, Byersdorfer CA, Boros L, Opipari AW.** 2014. Anaplerotic metabolism of alloreactive T cells provides a metabolic approach to treat graft-versus-host disease. J Pharmacol Exp Ther **351:**298–307. http://dx.doi.org/10.1124/jpet.114.218099.
66. **Duran RV, Oppliger W, Robitaille AM, Heiserich L, Skendaj R, Gottlieb E, Hall MN.** 2012. Glutaminolysis activates Rag-mTORC1 signaling. Mol Cell **47:**349–358. http://dx.doi.org/10.1016/j.molcel.2012.05.043.
67. **Thangavelu K, Pan CQ, Karlberg T, Balaji G, Uttamchandani M, Suresh V, Schuler H, Low BC, Sivaraman J.** 2012. Structural basis for the allosteric inhibitory mechanism of human kidney-type glutaminase (KGA) and its regulation by Raf-Mek-Erk signaling in cancer cell metabolism. Proc Natl Acad Sci U S A **109:**7705–7710. http://dx.doi.org/10.1073/pnas.1116573109.